



Acid functionalized carbon–silica composite and its application for solketal production



Devaki Nandan, Peta Sreenivasulu, L.N. Sivakumar Konathala, Manoj Kumar, Nagabhatla Viswanadham *

Catalytic Conversion Processes Division, CSIR-Indian Institute of Petroleum, Dehradun 248 005, India

ARTICLE INFO

Article history:

Received 18 December 2012
Received in revised form 20 May 2013
Accepted 4 June 2013
Available online 14 June 2013

Keywords:

Carbon–silica composite
Simultaneous carbonization sulfonation
Hierarchical mesopores
Solketal production

ABSTRACT

Various sulfonated carbon–silica-meso composite materials have been synthesized by adopting a novel concept of using glucose as a carbon source as well as precursor for the structure directing agent. The change in concentration of glucose in the initial gel mixture and the nature of treatment of the gel (thermal or hydrothermal methods) influenced the properties of the resultant composite material such as surface area, porosity and acidity. All the samples have been characterized by XRD, SEM, FT-IR, TPD, N₂ adsorption–desorption, CHNS elemental analysis and were used for acetalization of glycerol reaction to produce 2,2-dimethyl-1,3-dioxolane-4-methanol, also known as solketal. Among the various catalysts, the highly acidic composite gave the higher glycerol conversion (82%) and solketal selectivity. The activity achieved with sulfonated carbon–silica-meso composite was observed to be comparable with the reported results of known sulfonated catalyst Amberlyst-15. Optimal production of solketal over sulfonated carbon–silica-meso composite has been established at 70 °C reaction temperature after 30 min reaction time under reflux and the catalyst exhibited comparable activity at least up to the studied number of four cycles.

© 2013 Elsevier Inc. All rights reserved.

1. Introduction

Acidity is an important parameter in catalyst development, where the liquid acids such as H₂SO₄, HF and H₃PO₄ have been proven as efficient catalysts for various industrial processes by virtue of their higher K_a values and their efficient interaction with the reactant molecules. However, the toxicity and corrosive nature of the liquid acids are demanding alternative sources especially those of solid acids that are having advantage of easy separation from the product, reusability for recycle operation and their environment friendly nature [1–4]. But, the main limitation in using solid acids lies in their lower density and strength of acid sites. More over the accessibility of the reactant to the active sites and their stability in the aqueous environment need to be established. In order to take advantage of the positive aspects of liquid acids and solid acids, the method of immobilization of liquid acids onto the solid support, viz. sulfonation of activate carbon or metal oxides, came into practice in recent years that provides high acid functionality bearing solid materials for catalytic applications [5–6].

The acid functionalization of the solid support is generally carried out by three methods. The first method involves the immobilization of a thiol and sulfonate ester functional groups onto the mesoporous silica followed by oxidation of –SH to –SO₃H group

which also has its own limitation of low acid density [7–8]. The second method involves a single step co-condensation of tetraethyl-orthosilicate (TEOS) and 3-mercaptopropyl trimethoxysilane in the presence of block copolymer template. But, this method requires expensive template and 3-mercaptopropyl trimethoxysilane. Moreover, the block co-polymer needs to be leached out after the synthesis that makes the process multi-step and complicated due to its dependence on multiple factors. The third method involves two step process of carbonization of the carbon precursor or metal–carbon composite material followed by its sulfonation [9–12]. In present study, we have adopted a novel approach of simultaneous carbonization and sulfonation of glucose in the presence of organic silica (TEOS), where glucose act as cheaper carbon source as well as structure directing precursor through sulfonation for the formation of the acidic sulfonated carbon–silica-meso composite material (SCS) [13]. This work inspired us to study the role of various synthesis parameters such as the concentration of glucose, sulfuric acid and the method of treatment (thermal or hydrothermal) used for facilitating interaction between carbon and silica moiety in the SCS material. Here in we report the synthesis of various SCS materials exhibiting wide range of properties such as morphology, surface area, porosity and acidity that are expected to exhibit different catalytic properties. The composite material possessing high surface area and acidic properties is not only suitable for further functionalization with acid or metal ions but also provides good mechanical and thermal stability for catalytic applications.

* Corresponding author. Tel.: +91 135 2525856; fax: +91 135 2525702.
E-mail address: nvish@iip.res.in (N. Viswanadham).

The production of biodiesel is continuously gaining importance due to its biodegradable, non-toxic and renewable nature, which is relevant to the present scenario of call out for the alternative fuels to the traditional fossil fuels. The process of biodiesel formation involves transesterification reaction between vegetable oils or animal fats and methanol in the presence of an acid or a basic catalyst, where huge amount (~10 wt.%) of glycerol is produced as unavoidable bi-product [14–16]. The properties of glycerol such as diesel-immiscibility make it not suitable even for fuel blending and research is on for value addition of glycerol through its chemical conversion to useful products and to find new applications for this cheap and off grade glycerol obtained from biodiesel plants. Wide variety of chemicals and fuel blending stocks were reported to produce from glycerol through the chemical reactions [17–22]; selective oxidation for dihydroxyacetone, glyceraldehyde, glyceric acid, glycolic acid, hydroxypyruvic acid, mesoxalic acid, oxalic acid and tartronic acid; reduction for 1,3-propanediol and 1,2-propanediol; hydrogenolysis for propylene glycol; dehydration for acrolein or 3-hydroxypropionaldehyde; halogenation for 1,3-dichloropropanol; fermentation for 1,3-propanediol; polymerization for polyglycerols and polyglycerol esters (ESI† Table 1).

The production of oxygenates from glycerol gains much importance due to the excellent diesel-blending property of the oxygenates that not only improve the quality of the fuel but also increases the overall yield of the biodiesel in helping to meet the target for energy production from renewable sources for transport in the energy utilization directive. Olefins such as butene or alcohols such as tertiary butyl alcohol are commonly used as etherifying agents of glycerol, but the main drawback involved in the use of olefin is the formation of undesired di-olefins and the formation of huge amount of water in case of using alcohols [23–27]. Esterification with low molecular weight acids, transesterification with low molecular weight esters and acetalization with aldehydes or ketones are the other promising and economically viable alternative routes for the conversion of glycerol [28–32]. Acetalization with ketones, especially acetone is gaining importance due to the fact that acetone is widely produced from biomass conversion as well as from the chemical process of cumene cracking. Hence, facilitating reaction between two biomass derived products glycerol and acetone is advantageous as they constitute an excellent component for the formulation of gasoline, diesel and biodiesel fuels. These oxygenated compounds, when incorporated into standard diesel fuel, have led to a decrease in particles, hydrocarbons, carbon monoxide and unregulated aldehyde emissions. Likewise, these products also can act as improvers of cold flow and flash point properties of biodiesel along with simultaneous reduction its viscosity desirable for fuel applications [29].

The main challenge involved in glycerol acetalization is the production of water, which has to be removed in order to hinder the reversibility of the reaction. Continuous processes for the formation of solketal employing heterogeneous catalysts, such as the

commercial macro porous acid resins of the Amberlyst family, have been described by in the literature [28]. More recently, Vicente et al. [31] reported the suitability of sulfonic meso-structured silica as a catalyst for the acetalization of glycerol. Wider pores, large specific surface area, a relatively hydrophobic surface and the amount of accessible acid sites were identified as the factors that positively influence the catalytic performance in this reaction. However, the synthesis of material involved using costly organic template and multiple-step procedure. In the present study, we adopted a simple, single step, template-free, simultaneous carbonization and sulfonation method using glucose alone as carbon source as well as templating precursor, and explored the applicability of the SCS materials obtained in the synthesis for industrially important solketal production. Effect of synthesis variables such as glucose concentration was observed to alter the meso porosity of the materials in a significant manner.

In addition to the SCS materials, the study also focus on the synthesis of hierarchical mesoporous silica (HMS) exhibiting a range of porosity properties tuneable for the desired applications such as organic mass transformations, adsorption of gases and immobilization of different organic moieties and inorganic metals [33–35], by varying the glucose concentration in the initial synthetic mixture followed by the simple calcination of the SCS composite materials.

2. Experimental

2.1. Chemicals

Tetraethyl-orthosilicate (TEOS) was purchased from Merck, Germany. Glucose, sulfuric acid, glycerol and acetone was purchased from RFCL India private limited. All chemicals were used as received.

2.2. Synthesis of sulfonated carbon-silica-meso composite materials

Two different methods have been adopted for the synthesis of various sulfonated carbon silica composite materials. While both the methods follow the similar procedure and composition of the gel precursors, the main difference lies in adopting thermal or hydrothermal treatment for controlling extent of interaction between carbon and silicon species. In a typical synthesis procedure, a solution obtained by dissolving 20 g of glucose in 20 g de-ionized water was added drop-wise to the 60 g TEOS solution, followed by drop-wise addition of 23 g of concentrated sulfuric acid (98%). Special care has taken to control the temperature (very slow addition of the acid) of the solution while adding the sulfuric acid. The solutions were continuously under vigorous stirring throughout the procedure and the resultant mixture was further allowed for mixing under stirring for 3 h. The synthesis procedure is common in both the methods up to this stage while the procedure differs in the following steps. In the thermal treatment method, the dry gel

Table 1
Textural properties of the synthesized materials.

Sample	SA_{BET} (m^2g^{-1a})	SA_{mi} (m^2g^{-1b})	SA_{mc} (m^2g^{-1c})	% SA_{mc}	V_{tot} (cm^3g^{-1d})	V_{mi} (cm^3g^{-1e})	D (nm^f)
SCS1/0.3	779	240	539	69.19	0.52	0.10	2.6
SCS1/1	426	166	260	61.03	0.61	0.07	5.6
SCS1/2	425	274	151	35.52	0.32	0.11	3.0
HSCS1/0.3	238	21	217	91.17	0.82	0.0072	13.8
HSCS1/1	176	82	94	53.40	0.25	0.039	5.9
HSCS1/2	242	119	123	50.82	0.35	0.0497	5.7

^a BET surface area.

^b Micropore surface area calculated from t -plot [38–40].

^c Mesopore surface area were calculated as $SA_{BET} - SA_{mi}$.

^d Total pore volume taken from the volume of N_2 adsorbed at $P/P_0 = 0.995$.

^e Micropore volume calculated from t -plot.

^f BJH adsorption average pore diameter.

thus obtained was transferred to silica crucible and was heated at 120 °C inside oven having air circulation for 12 h. On the other hand, in the second method the gel obtained in the first step was treated inside the Teflon-lined autoclave at 150 °C for 15 h for hydrothermal synthesis. The ramping method is used to achieve the temperature (150 °C) maintained by P.I.D. Controller, where the gradual raise in temperature was carried out with the rate 2.5 °C per minute and the targeted temperature of 150 °C was achieved in 1 h. The third step is common in both the methods, wherein the resultant solid black mass was treated at 300 °C for 4 h under nitrogen atmosphere to obtain the solid form of sulfonated carbon–silica-meso composite material. The materials were washed with ample amount of cold – followed by hot deionized water until no sulfate ions appeared in filtrate solution (by checking with barium hydroxide solution) and dried at 120 °C temperature for 12 h. The materials synthesized by first method are denoted as sulfonated carbon–silica-meso composite (SCS) and the materials synthesized by second method are denoted as hydrothermally treated sulfonated carbon–silica-meso composite (HSCS). Since, glucose is the carbon source as well as structure directing agent, the concentration of glucose is varied in both the methods to understand its role in the carbonization and final properties of the materials. The materials thus obtained are denoted as SCS1/0.3, SCS1/1, SCS1/2, HSCS1/0.3, HSCS1/1 and HSCS1/2, where the numeric value indicates the weight ratio of TEOS/glucose taken in the synthesis mixture. Since, the use of sulfuric acid is for the sulfonation of the carbon moiety, the molar ratio of glucose to sulfuric acid was kept constant for the synthesis of all the materials. The SCS and HSCS samples synthesized by the above mentioned methods are acted as potential source for the production of hierarchical mesoporous silica (MS) materials that are formed by simple calcination of the SCS/HSCS at 600 °C for 10 h.

2.3. Characterization

Powder X-ray diffraction patterns of the samples were recorded on a Regaku Dmax III B equipped with rotating anode and CuK α radiations. SEM images were recorded for obtaining particle morphology on Quanta 200f instrument, Netherland. Nitrogen sorption isotherms were obtained using micromeritics ASAP 2010 unit, USA, operated at –203 °C, where the samples were degassed at 250 °C prior to measurement of specific BET surface area and pore volume. Pore size was calculated from the desorption branch of the adsorption–desorption isotherms by the Barrett–Joyner–Halenda (BJH) method. TPD of the samples were recorded in micromeritics 2010 unit, USA, where helium is used as carrier gas and prior to the ammonia adsorption the samples were degassed at 250 °C for one hour. Thermo gravimetric analyses (TGA) of these samples were carried out for the temperature range of 30–800 °C under the nitrogen flow. The IR spectra of the both samples were recorded on Thermo Nicolet 8700 instrument, Thermoscientific Corporation, USA. The reaction products are analyzed by using GC equipped with the DB wax column and FID detector. The total acidity was determined by treatment of each catalyst with concentrated NaCl solution and filtrate was titrated by NaOH solution.

2.4. Application of materials for solketal synthesis

All the synthesized materials were used for acetalization of glycerol with acetone to yield solketal. In a typical experiment, 0.25 g of catalyst (5% of glycerol weight) was taken in a round bottom flask and 18.91 g of acetone and 5 g of glycerol with glycerol to acetone molar ratio 1:6 was added to it and the mixture was refluxed at 70 °C for different time duration viz. from 30 min to 4 h. After reaction was completed products were analyzed by GC.

3. Results and discussion

Carbonization and sulfonation are the two important steps that influence the nature and properties of the sulfonated carbon–silica composite materials. The rate and extent of carbonization also influence the amount of sulfonyl bearing groups on the carbon moiety which are related with the acidity of the final material. Due to these reasons, the strategy adopted in the present study is related to the change in concentration of the carbon precursor, glucose and the conditions to facilitate effective interaction between carbon and silicon species during the simultaneous carbonization and sulfonation synthesis. The variation in glucose concentration is also expected to alter the material quality due to the fact of the structure directing property of its intermediate species. To know the effect of glucose on the properties of materials such as acidity, porosity and surface area we have varied the glucose concentration while keeping the TEOS concentration constant. Further, to facilitate the effective interaction between carbon and silicon species, we have adopted additional step of hydrothermal treatment of the reaction mixture so as to improve the simultaneous sulfonation and carbonization.

3.1. Effect of synthesis conditions on material properties

The influence of synthesis conditions, such as the amount of glucose and concentration of sulfuric acid, on the morphology of SCS, HSCS are investigated. The SEM images of the samples prepared by varying glucose concentration and synthesis method have been given in Fig. 1. The SCS samples synthesized by thermal method exhibited non-uniform (hierarchical) morphology of agglomerated spheres in the composite, while those of hydrothermally synthesized samples (HSCS) appeared in uniform spherical morphology. Among the hydrothermally treated samples, the sample HSCS 1/0.3 exhibits smoothly surfaced spherical agglomerates that may be due to the excess amount of silica species that superfluous to generate sufficient primary silica particles on the surface besides its interaction with carbon in the carbon silica composite material. At higher glucose concentrations the material (HSCS1/2) exhibited cracked sphere morphology that is attributed to the formation of thinner outer shell prone to breakage. The above results demonstrated that the shell morphology of composite material could be easily controlled by adjusting the ratio of glucose to silica concentration. However, a commonality observed in both the methods (SCS as well as HSCS) is the increase in agglomerate size with glucose concentration. The IR spectra of the samples show the interaction between silica and carbon moiety in both SCS and HSCS materials (Fig. 2A and B). It is known that sulfonated carbon exhibits two characteristic bands representing the –OSO₃H group at 1712 cm^{–1} and 1207 cm^{–1} [36]. In our study, all the SCS and HSCS samples also exhibited a band at 1712 cm^{–1}, but the second one at 1207 cm^{–1} is not distinct as it is merged with the band at 1090 cm^{–1} related to silica. Further as the synthesis of material was carried out in air, there is a fair chance for the oxidation of glucose in presence of concentrated sulfuric acid to form the –COOH groups. Thus, the band at 1712 cm^{–1} obtained for the materials may also due to stretching vibration of (C=O) of –COOH group. The additional bands obtained at 3447 cm^{–1} and 803 cm^{–1} are due to presence of –OH and SiO₂ stretching, Vibrations. The presence of aromatic carbon is confirmed by the presence of band at 1620 cm^{–1}.

3.2. Porosity and acidic properties of the synthesized materials

Small angle X-ray diffraction patterns of the samples (ESI Fig. 1) reveal the presence of larger meso-porosity in the synthesized

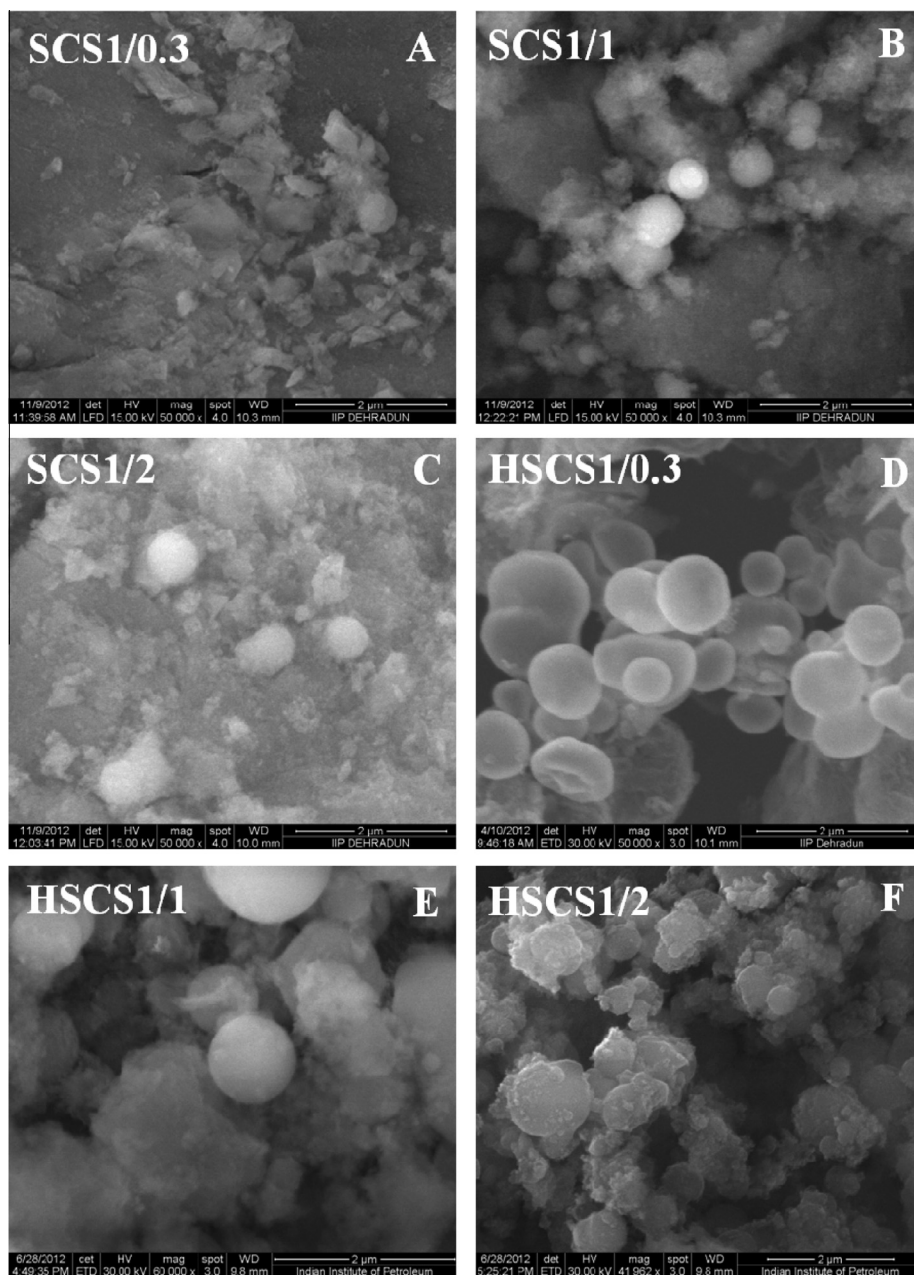


Fig. 1. SEM images of the materials synthesized by thermal method (A, B and C) and hydrothermal methods (D, E and F).

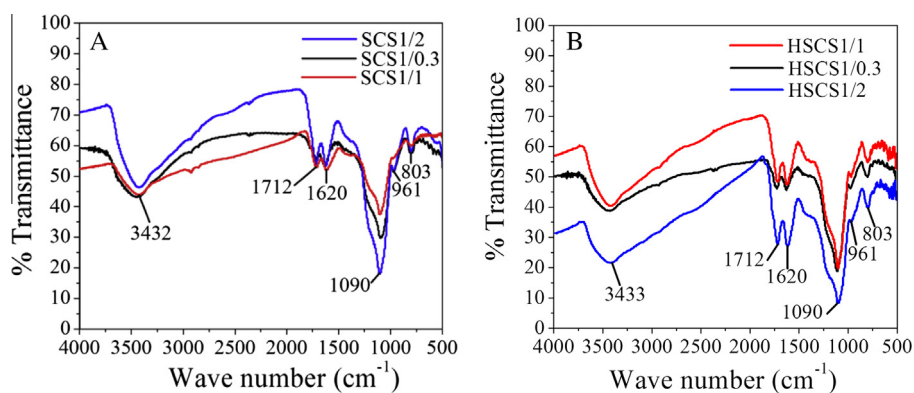


Fig. 2. FT-IR spectra of synthesized materials (A) SCS and (B) HSCS.

materials [37]. Textural properties of the materials given in Table 1 reveal that the materials synthesized by thermal method (SCS) exhibit higher surface area and micropore surface areas compared to those synthesized by hydrothermal method (HSCS). However, a common feature observed in both SCS and HSCS materials is the increase in the micropore surface area with the glucose concentration that is indeed expected from the formation of more microporous carbon material with increasing carbon source, glucose in the synthesis mixture. Accordingly, except SCS 1/1, the percentage of mesoporous surface area is lower in SCS materials (Table 1). The nitrogen adsorption–desorption isotherms of SCS samples (Fig. 3A) indicate that the hysteresis loop representing mesopores is not H1 type (observed for larger mesopores) in SCS1/0.3, but it is shifted to H1 type with increasing glucose concentration (as in case of SCS1/1 and SCS1/2). In SCS 1/0.3 the hysteresis loop was broad with range of nitrogen adsorption volume from 0.2 to 0.7 P/P_0 (relative pressures) signifying the presence of small mesopores. But in case of SCS1/1 the hysteresis loop representing the range of nitrogen adsorption volume shifted to higher level (0.6–1.0 P/P_0) signifying the presence of mesoporosity with larger mesopores [37]. However, further increase of glucose concentration as in case of SCS1/2 could not continue this increase rather decrease in area of hysteresis loop was observed. There seems an optimum amount of glucose required in SCS material, for its effective interaction with silica species to form larger pores where, the concentration of glucose used in SCS1/1 (with equal wt. ratios of glucose and TEOS) produced the material with best porosity properties. This phenomenon is also supported by the pore size distribution of corresponding samples (Fig. 3B) where the average pore diameter of SCS1/0.3 was 2.6 nm which is initially increased with glucose concentration to 5.6 nm in SCS1/1, while further increase in glucose concentration resulted in reversible effect of decrease in the size to 3 nm in SCS1/2 sample. Overall, sample SCS1/1 exhibited superior properties in terms of porosity and average pore

size. Unlike this, all the three materials synthesized by hydrothermal method (HSCS) exhibited uniform pores of type IV with H1 type hysteresis loop configuration representing the larger mesopores (Fig. 3C). The presence of larger mesoporosity was evident from the sharp uptakes of nitrogen volume adsorbed at relative pressures of 0.7–0.10 P/P_0 as a result of capillary condensation inside the mesopores in HSCS1/0.3. Increase in the glucose concentration resulted in significant change in loop configuration where the area inside the loop is decreased in both HSCS1/1 and HSCS1/2 samples. This phenomenon is also supported by pore size distribution of the corresponding materials (Fig. 3D) where ordered and larger mesopores are formed (average pore diameter (13.8 nm) at low glucose (SCS1/0.3) concentrations. But, increase in glucose concentration resulted in change from ordered mesopores to hierarchical mesopores of lower pore diameter (average pore diameter of 5.7–5.9 nm), and the hierarchy of the pores is further increased with glucose concentration (HSCS1/2). It is interesting to see, at same glucose concentrations, the materials synthesized by hydrothermal method exhibited larger pore diameter. For example, the average pore diameter of the HSCS1/0.3 is 13.8 nm against 2.6 nm of the SCS1/0.3.

The properties of HMS samples obtained by simple calcination of corresponding composite material (for removal of carbon moiety ESI Table 2) indicates that average pore diameter as well as the percentage of meso pore surface area of the materials increased after the removal of carbon moiety. This observation suggests that the carbon moiety is surrounded by silica moiety in the composite material. Further, increase of glucose concentration in the initial gel resulted in increase in average meso pore diameter of the resultant HMS.

The acidity of the samples is measured by three methods; temperature programmed desorption of ammonia (Fig. 4), acid–base titration, elemental sulfur analysis (Table 2) and EDX analysis (ESI Fig. 2). The common trend of increase in acidity of the

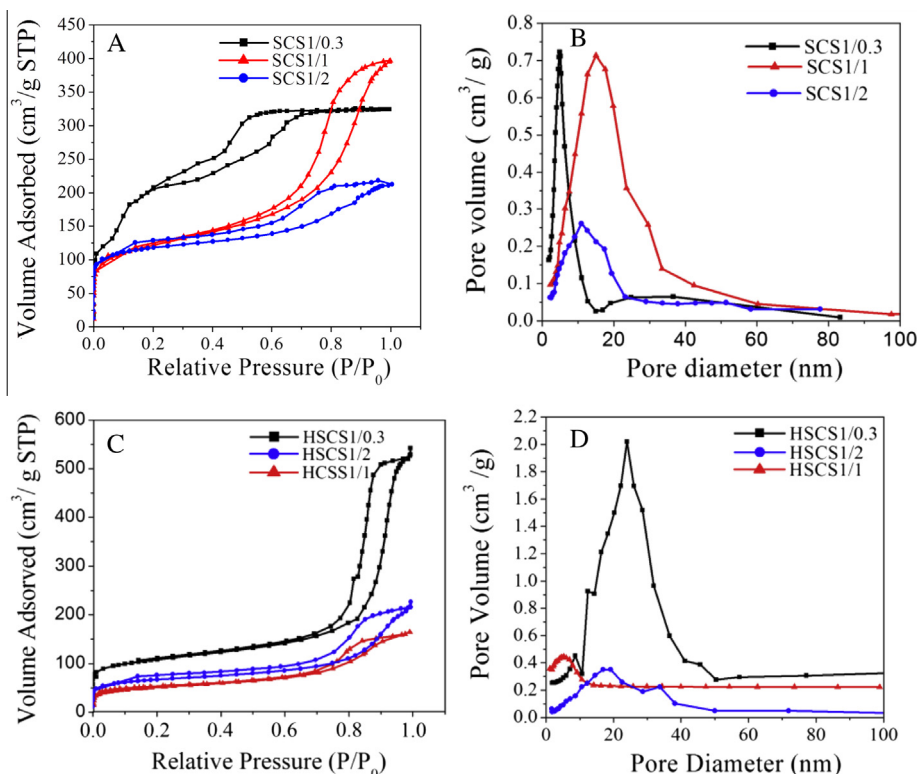


Fig. 3. (A) and (C) N₂ adsorption-desorption isotherms of the samples of SCS and HSCS, respectively (B) and (D) is the respective pore size distribution using BJH method.

Table 2

Elemental composition and acid density of the synthesized materials.

Sample	Carbon (%)	Hydrogen (%)	Sulfur (%)	Acid density due to $-\text{SO}_3\text{H}$ (mmol/g) ^a	Total acid density (mmol/g) ^b
SCS1/0.3	22.96	1.93	0.36	0.11	0.90
SCS1/1	30.59	1.79	0.45	0.14	1.20
SCS1/2	48.28	2.18	0.58	0.18	1.35
HSCS1/0.3	25.70	1.45	0.20	0.06	1.05
HSCS1/1	33.38	1.86	0.21	0.06	1.50
HSCS1/2	42.53	1.58	0.23	0.07	2.25

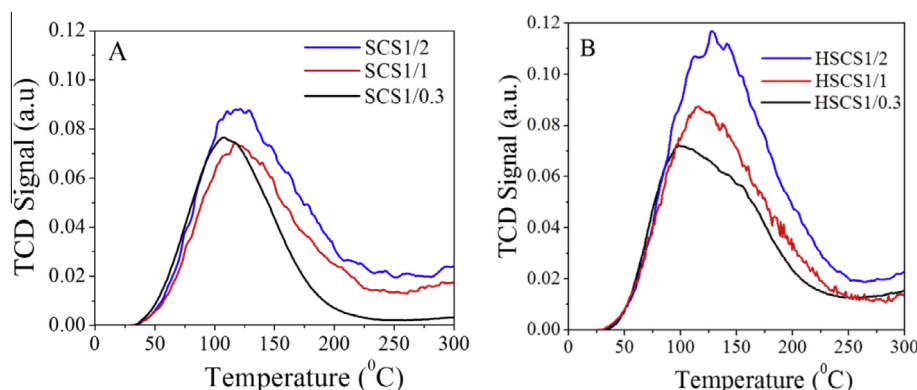
^a Calculated from sulfur content assuming all S atoms are in the SO_3H form.^b Determined by acid base titration.

composite materials with the glucose concentration was observed for all the samples. Further, the acidity related to $-\text{SO}_3\text{H}$ groups of the samples is lower than the total acidity measured by titration method. This may be due to the contribution of other functional groups ($-\text{COOH}$, phenolic $-\text{OH}$), which is supported by IR analysis. But, the only difference observed between the properties of the materials synthesized by two methods is the increase in acidity is significant in the materials synthesized by hydrothermal method (HSCS) when compared to those synthesized by thermal method (SCS). Further the TGA analysis of the composite materials synthesized by thermal and hydrothermal methods (Fig. 5) shows weight loss at two places: (1) below 100°C due to the removal of moisture and (2) between 300°C and 750°C due to the removal of carbon material from the composite. The above discussion envisions that the catalysts are stable at the chosen reaction temperature i.e. 70°C under solvent free conditions.

3.3. Plausible mechanism for the formation of SCS, HSCS and HMS materials

Based on the surface area and porosity, morphology of the materials obtained by SEM images and acidity trends observed in TPD analysis of the composite materials we have proposed a schematic model for the formation of SCS and HSCS materials obtained by thermal and hydrothermal routes (Fig. 6). The TEOS and Glucose undergo hydrolysis in presence of sulfuric acid to produce the silica and carbon species in the first step, which is common in both thermal and hydrothermal methods. However, the direct interaction between lyophilic carbon species and hydrophilic silica species is not possible. Here, sulfuric acid can act as sulfonation agent and the interaction of sulfuric acid with unsaturated cyclic carbon moiety creates the polarity in the molecule. This supramolecular assembly of glucose molecules helps to form the cage-like structure inside the SiO_2 , where otherwise difficult interaction between hydrophobic carbon moiety and hydrophilic silica moiety is facilitated by the presence of hydrophilic $-\text{SO}_3\text{H}$ functional groups on the hydrophobic carbon moiety for the successful formation of

the composite [41–42]. In the present synthesis, there is no structure directing agent is used in the initial gel mixture, but the sulfonyl carbon species formed by the sulfuric acid treatment of glucose in the initial gel itself acts as structure directing agent and its further interaction with silica species facilitates the formation of mesopores (carbon–silica–composite material). Hence, the high amount of mesopores formed in the hydrothermal method gives indirect evidence to the better interaction between carbon and silica moiety. The extent of carbonization of the carbon moiety and its interaction with silica moiety is strongly influenced by the concentration of sulfonyl group functionalized on the carbon moiety. Hence, the key factor in the synthesis of composite material seems to be governed by the carbonization and sulfonation reactions, where thermal and hydrothermal methods adopted (in the second step of the synthesis) in the present study were observed to influence the properties of the material. As shown in Fig. 6, compared to thermal method, the hydrothermal method adopted in step 2 of the synthesis facilitates effective sulfonation of the carbon moiety due to the presence of the autogenous pressure created in the autoclave that results in enhanced interaction between carbon and silicon moieties. Third step is common in both the methods, where the solid materials obtained in the second step are treated at high temperatures under nitrogen atmosphere for the complete carbonization of the materials to obtain sulfonyl functionalized thermally stable carbon–silica composite materials. As shown in Fig. 6, the carbonization step yields different type of materials in two different methods, where, the effective interaction of sulfonyl groups with carbon moiety facilitated in hydrothermal method yields homogeneously distributed sulfonyl interacted carbon–silica composite (HSCS) with larger mesopores, while the thermal method results in the formation of heterogeneously distributed carbon having localized carbon moieties along with silicon interacted carbon responsible for formation of considerable micropores and smaller mesopores in SCS materials. The fourth and final step is the production of mesoporous silica from the composite materials by thermal treatment to remove the carbon moiety in the composite material, where both HSCS and SCS materials produced

**Fig. 4.** TPD spectra of synthesized (A) SCS and (B) HSCS materials.

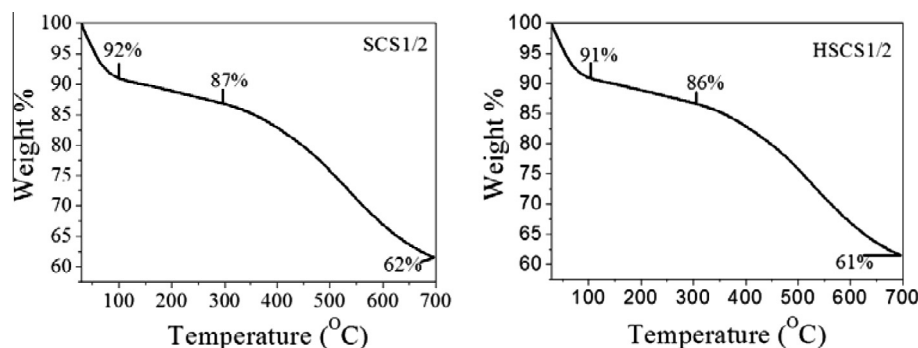


Fig. 5. TGA spectra of synthesized (A) SCS and (B) HSCS materials.

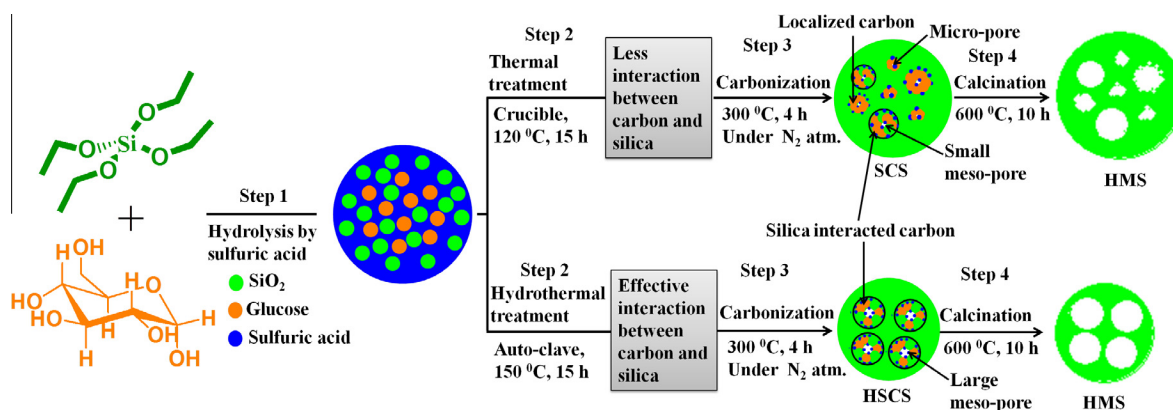


Fig. 6. Plausible mechanism for the formation of SCS, HSCS and HMS materials.

hierarchical mesoporous silica (HMS), with only difference of producing larger mesopores in hydrothermal method and smaller mesopores in thermal method.

From above discussions the hydrothermal method seems to be better to synthesize the composite material (HSCS) with larger mesopores and higher acidity required for the catalytic transformation of bulky molecules. However, the presence of micropores and the low diameter mesopores in SCS 1/0.3 resulted in high surface area of this material. Hence, this material also exhibits lower average pore diameter values that further confirm the presence of carbon/carbon–silica inside the silica shell which finds applications in catalysis due to its high surface area and hierarchical porosity.

3.4. Catalytic application of SCS and HSCS materials

All the composite materials synthesized in this study have been tested for glycerol to solketal reaction under similar conditions by taking reactant mixture in the round bottomed flask attached with reflux condenser at 70 °C reaction temperature and glycerol/acetone molar ratio of 1/6. Among the various catalysts, the highest glycerol conversion of 82% along with 99% selectivity to solketal was obtained over the HSCS1/2 (Table 3). In a typical reaction conducted on HSCS1/2 indicated the gradual increase of conversion from 30% to 82 up to the reaction time of 30 min and the conversion levels are stabilized and no further change in these values observed with reaction time (Fig. 7). A blank reaction conducted in the absence of catalyst ascertained that there is no production of solketal. Hence the reaction time of 30 min is considered for equilibrium attainment of the reaction and the product is collected after this time period on all the catalysts. The highest conversion of glycerol observed on HSCS1/2, despite of its lower porosity

and low surface area indicate that the mesopores size alone is not responsible for the catalytic activity of these composite materials. Since, the reaction under study is of acid catalyzed nature, the catalytic activity of the materials may be related with the acidity of the samples. The acidity patterns given in TPD spectra and total acidity measured by NaOH titration indeed indicate the highest activity exhibiting sample HSCS1/2 also exhibits highest acidity that supports the direct role of acidity in catalytic activity. All other composite materials also exhibited the higher conversion values of >75% (lower when compared to HSCS1/2) of glycerol. A general trend observed in catalytic activity is that the hydrothermally treated composite materials (HSCS) outperformed the corresponding samples prepared by thermal method (SCS) at all the glucose concentrations. This may be due to the higher total acid density and larger mesopore formation facilitated in the hydrothermal treatment method. However TOF values calculated for HSCS samples

Table 3

Catalytic activity and product distribution with time.^a

Catalyst	Conversion (%)	Solketal sel. (%)	TOF/h ^b
SCS1/0.3	76	95	39
SCS1/1	79	76	37
SCS1/2	75	90	30
HSCS1/0.3	79	98	35
HSCS1/1	80	98	32
HSCS1/2	82	99	30
Amberlyst-15 ³¹	85.1	–	

^a 0.25 g of catalyst (5% of glycerol weight) was taken in a round bottom flask and 18.91 g of acetone and 5 g of glycerol with glycerol to acetone molar ratio 1:6 was added to it and reflux at 70 °C for 30 min.

^b TOF value is based on the moles of the glycerol converted per mole of total acid site per h.

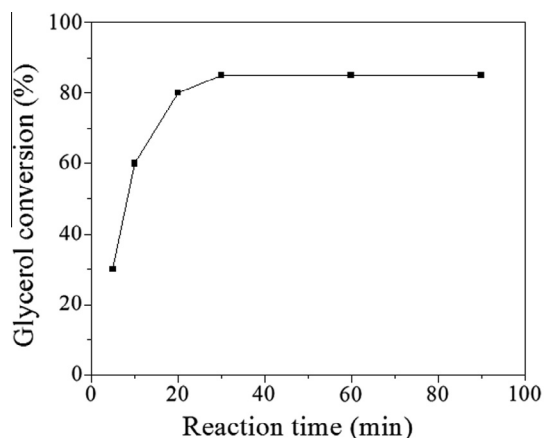


Fig. 7. Performance of a typical composite catalyst with reaction time.

Table 4
Recycling experiments on the HSCS1/2 catalyst for the synthesis of solketal.^a

Run	Glycerol conversion	Total acid density (mmol/g) ^b
1	82	2.25
2	80	2.20
3	81	2.19
4	79	2.15

^a 0.25 g of catalyst (5% of glycerol weight) was taken in a round bottom flask and 18.91 g of acetone and 5 g of glycerol with glycerol to acetone molar ratio 1:6 was added to it and reflux at 70 °C for 30 min.

^b Acidity was determined by acid base titration.

are comparable with those of the SCS samples (Table 3). Further, the performances of HSCS materials are also comparable with those reported for sulfonic acid modified silica catalysts (82.5% for Ar-SBA-15 and 79.0% Pr-SBA-15) (Table 3). However the performances of the catalysts are not directly correlated with the amount of sulfur estimated by elemental analysis. This may be due to the contribution of –COOH and phenolic –OH groups (in addition to –SO₃H) to the total acidity. This is in accordance with the results reported for the sulfonated carbon catalysts [43–44]. Further, the co-presence of the hydrophilic –COOH and phenolic –OH groups in the HSCS materials of the present study may also play an important role in promoting the activity of the catalyst by creating strong affinity between the hydrophilic parts of the reactants with the catalyst. Thus the presence of acidic SO₃H groups along with hydrophilic groups (–COOH and –OH) present in composite material of present study provides a beneficial factor for the development of the catalytic process for solketal production, and the catalyst also exhibits constant glycerol conversion up to the 4 reaction cycles (Table 4).

4. Conclusions

The synthesis of sulfonated carbon–silica–meso composite materials with tuneable acidity and porosity are reported for first time by adopting simple one step method of simultaneous carbonization and sulfonation. The simplicity involved in the material synthesis using low cost glucose as a carbon source as well as structure directing precursor makes the present method novel to those relevant works reported in the prior art. The materials exhibited excellent catalytic activity in the acetalization of acetone with a renewable feedstock, glycerol to produce 2,2-dimethyl-1,3-dioxolane-4-methanol (solketal) thus provides an efficient heterogeneous catalyst for the value addition of the undesired bi-product glycerol obtained in the biodiesel synthesis. The glycerol conver-

sion and product selectivities achieved on these materials are comparable to those reported for other sulfonated materials. Moreover, the active mesoporous materials do not suffer from leaching problems and can be efficiently reused in consecutive catalytic cycles. The synthesized SCS materials and the mesoporous silica (MS) obtained by carbon removal through simple calcination of SCS exhibit different porosity and can be used as catalysts and supports for vivid catalytic applications.

Acknowledgments

Authors are thankful to the director, IIP, for his encouragement. DN and PS acknowledge CSIR, New Delhi, for awarding fellowship. We are thankful to XRD, IR, Porosimetry, and SEM, groups at IIP for analysis.

Appendix A. Supplementary data

Supplementary data associated with this article can be found, in the online version, at <http://dx.doi.org/10.1016/j.micromeso.2013.06.004>.

References

- [1] M. Toda, A. Takagaki, M. Okamura, N.N. Kondo, S. Hayashi, K. Domen, M. Hara, *Nature* 438 (2005) 178.
- [2] S. Suganuma, K. Nakajima, M. Kitano, D. Yamaguchi, H. Kato, S. Hayashi, M. Hara, *J. Am. Chem. Soc.* 130 (2008) 12787–12793.
- [3] M. Kitano, D. Nakajima, M. Kitano, D. Yamaguchi, H. Kato, S. Hayashi, M. Hara, *Langmuir* 25 (2009) 5068–5075.
- [4] Yamaguchi, M. Kitano, S. Suganuma, K. Nakajima, H. Kato, M. Hara, *J. Phys. Chem. C* 113 (2009) 3181–3188.
- [5] S.Y. Chen, T. Yokoi, C.Y. Tang, L.Y. Jang, T. Tatsumi, J.C.C. Chana, S. Cheng, *Green Chem.* 13 (2011) 2920–2930.
- [6] J. Peng, L.P. Mo, F.Y. Zhao, L.L. Hpu, L. Yang, Z.H. Zhang, *Green Chem.* 13 (2011) 2576–2584.
- [7] D. Margolese, J.A. Melero, S.C. Christiansen, B.F. Chmelka, G.D. Stucky, *Chem. Mater.* 12 (2000) 2448–2459.
- [8] A. Karam, J.C. Alonso, T.I. Gerganova, P. Ferreira, N. Bion, J. Barrault, F. Jérôme, *Chem. Commun.* (2009) 7000–7002.
- [9] P. Gupta, S. Paul, *Green Chem.* 13 (2011) 2365–2372.
- [10] S. Van de Vyver, L. Peng, J. Geboers, H. Schepers, F. De clippel, C.J. Gommès, B. Goderis, P.A. Jacobs, B.F. Sels, *Green Chem.* 12 (2010) 1560–1563.
- [11] X. Mo, E. Lotero, C. Lu, Y. Liu, J.G. Goodwin, *Catal Lett.* 123 (2008) 1–6.
- [12] L. Peng, A. Philippaerts, X. Ke, J.V. Noyen, F.D. Clippel, G.V. Tendeloo, P.A. Jacobs, B.F. Sels, *Catal. Today* 150 (2010) 140–146.
- [13] D. Nandan, P. Sreenivasulu, S.K. Saxena, N. Viswanadham, *Chem. Commun.* 47 (2011) 11537–11539.
- [14] B. Freedman, E.H. Pryde, T.L. Mounts, *J. Am. Oil Chem. Soc.* 61 (1984) 1638–1643.
- [15] T. Werpy, G. Petersen, In *Top Value Added Chemicals From Biomass*, the Pacific Northwest National Laboratory (PNNL) and the National Renewable Energy Laboratory (NREL), U.S. Department of Energy, 2004.
- [16] European Biodiesel Board, <http://www.ebb-eu.org/index.php>.
- [17] M. Pagliaro, R. Ciriminna, H. Kimura, M. Rossi, C. Della Pina, *Angew. Chem. Int. Ed.* 46 (2007) 4434–4440.
- [18] C. Zhou, J.N. Beltrami, Y. Fana, G.Q. Lu, *Chem. Soc. Rev.* 37 (2008) 527–549.
- [19] Y. Zheng, X. Chen, Y. Shen, *Chem. Rev.* 108 (2008) 5253–5277.
- [20] A. Behr, J. Eilting, K. Irawadi, J. Leschinski, F. Lindner, *Green Chem.* 10 (2008) 13–30.
- [21] Y. Gu, A. Azzouzi, Y. Pouilloux, F. Jérôme, J. Barrault, *Green Chem.* 10 (2008) 164–167.
- [22] A. Corma, S. Iborra, A. Velty, *Chem. Rev.* 107 (2007) 2411–2502.
- [23] H. Nouredini, U.S. Patent 6015 440, 2000.
- [24] H. Nouredini, U.S. Patent 6174 501, 2001.
- [25] K. Klepacova, D. Mravec, A. Kaszonyi, M. Bajus, *Appl. Catal. A* 328 (2007) 1–13.
- [26] J.A. Melero, G. Vicente, G. Morales, M. Paniagua, J.M. Moreno, R. Roldán, A. Ezquerro, C. Pérez, *Appl. Catal. A* 346 (2008) 44–51.
- [27] N. Viswanadham, S.K. Saxena, *Fuel* 103 (2013) 980–986.
- [28] J. Deutsch, A. Martin, H. Lieske, *J. Catal.* 245 (2007) 428–435.
- [29] E. García, M. Laca, E. Pérez, Á. Garrido, J. Peinado, *Energ. Fuels* 22 (2008) 4274–4280.
- [30] C.X. Da Silva, V.L. Gonçalves, C.J. Mota, *Green Chem.* 11 (2009) 38.
- [31] G. Vicente, J.A. Melero, G. Morales, M. Paniagua, E. Martín, *Green Chem.* 12 (2010) 899.
- [32] M. Selva, V. Benedet, M. Fabris, *Green Chem.* 14 (2012) 188–200.
- [33] K. Komura, Y. Nakano, M. Koketsu, *Green Chem.* 13 (2011) 828–831.

- [34] A.M.B. Furtado, J. Liu, Y. Wang, M.D. LeVan, *J. Mater. Chem.* 21 (2011) 6698–6706.
- [35] F. Rascón, R. Wischert, C. Copéret, *Chem. Sci.* 2 (2011) 1449–1456.
- [36] M.H. Zong, Z.Q. Duan, W.Y. Lou, T.J. Smith, H. Wu, *Green Chem.* 9 (2007) 434–437.
- [37] Z. Niu, S. Kabisatpathy, J. He, L.A. Lee, J. Rong, L. Yang, G. Sikha, B.N. Popov, T.S. Emrick, T.P. Russell, Q. Wang, *Nano Res.* 2 (2009) 474–483.
- [38] J.H. de Boer, A.V. Heuvel, B.G. Linsen, *J. Catal.* 3 (1964) 268–273.
- [39] J.H. de Boer, B.C. Lippens, *J. Catal.* 3 (1964) 38–43.
- [40] B.C. Lippens, J.H. de Boer, *J. Catal.* 3 (1964) 44–49.
- [41] J.H. Pan, H. Dou, Z. Xiong, C. Xu, J. Ma, X.S. Zhao, *J. Mater. Chem.* 20 (2010) 4512–4528.
- [42] D. Chen, F. Huang, Y.B. Cheng, R.A. Caruso, *Adv. Mater.* 21 (2009) 2206–2210.
- [43] M. Hara, *Top Catal.* 53 (2010) 805–810.
- [44] L. Geng, Y. Wang, G. Yu, Y.X. Zhu, *Catal Comm.* 13 (2011) 26–30.